

## Error reduction in EMG signal decomposition

Joshua C. Kline<sup>1,2</sup> and Carlo J. De Luca<sup>1,2,3,4,5,6</sup>

<sup>1</sup>NeuroMuscular Research Center, Boston University, Boston, Massachusetts; <sup>2</sup>Department of Biomedical Engineering, Boston University, Boston, Massachusetts; <sup>3</sup>Department of Electrical and Computer Engineering, Boston University, Boston, Massachusetts; <sup>4</sup>Department of Neurology, Boston University, Boston, Massachusetts; <sup>5</sup>Department of Physical Therapy, Boston University, Boston, Massachusetts; and <sup>6</sup>Delsys, Natick, Massachusetts

Submitted 7 October 2013; accepted in final form 8 September 2014

**Kline JC, De Luca CJ.** Error reduction in EMG signal decomposition. *J Neurophysiol* 112: 2718–2728, 2014. First published September 10, 2014; doi:10.1152/jn.00724.2013.—Decomposition of the electromyographic (EMG) signal into constituent action potentials and the identification of individual firing instances of each motor unit in the presence of ambient noise are inherently probabilistic processes, whether performed manually or with automated algorithms. Consequently, they are subject to errors. We set out to classify and reduce these errors by analyzing 1,061 motor-unit action-potential trains (MUAPTs), obtained by decomposing surface EMG (sEMG) signals recorded during human voluntary contractions. Decomposition errors were classified into two general categories: location errors representing variability in the temporal localization of each motor-unit firing instance and identification errors consisting of falsely detected or missed firing instances. To mitigate these errors, we developed an error-reduction algorithm that combines multiple decomposition estimates to determine a more probable estimate of motor-unit firing instances with fewer errors. The performance of the algorithm is governed by a trade-off between the yield of MUAPTs obtained above a given accuracy level and the time required to perform the decomposition. When applied to a set of sEMG signals synthesized from real MUAPTs, the identification error was reduced by an average of 1.78%, improving the accuracy to 97.0%, and the location error was reduced by an average of 1.66 ms. The error-reduction algorithm in this study is not limited to any specific decomposition strategy. Rather, we propose it be used for other decomposition methods, especially when analyzing precise motor-unit firing instances, as occurs when measuring synchronization.

surface EMG signal; decomposition; motor-unit firing instances; accuracy; error reduction

OVER THE PAST FIVE DECADES, a variety of methods have been used to extract individual motor-unit action potentials (MUAPs) from electromyographic (EMG) signals. Manual decomposition techniques were the first methods used to extract the firing instances of one or two MUAP trains (MUAPTs) by visual inspection of the signal. Still used today, generally, these methods are incapable of resolving MUAP superpositions that occur in complex EMG signals. Therefore, manual decomposition is, by necessity, limited to indwelling EMG signals from low-force contractions, where few motor units are active. The introduction of automated algorithms, using various machine-learning processes, enabled the decomposition of indwelling EMG signals having a more complex structure (Florestal et al. 2006; LeFever and De Luca 1982a, b; McGill et al. 2004; Nawab et al. 2008). More recent enhancements allow for the

decomposition of complex surface EMG (sEMG) signals that can identify the activity of superimposed MUAPs (De Luca et al. 2006; Holobar and Zazula 2007; Kleine et al. 2007; Nawab et al. 2010).

Regardless of the method used, decomposition of EMG signals, containing the MUAPs of any number of motor units, is a nontrivial task, with the task increasing in complexity as the number of active motor units and the noise in the signal increase. Even if the decomposition is performed manually, the low contraction levels used in such studies often contain some superposition occurrences, causing difficulty in resolving precise firing instances. As a consequence of the variability in decomposition results, any decomposition process (automatic or manual) provides only probabilistic estimates of physiological motor-unit firing instances corrupted by two types of decomposition errors: “Location error” and “Identification error.”

Figure 1 shows an example of these error manifestations. One type of error occurs when the firing instances of one MUAP are either missed or falsely detected, due to confusion with another MUAP of similar shape (Fig. 1A). These errors are visible when a validation of the first decomposition is performed, and false positives or false negatives occur for the same motor unit. We refer to these as Identification errors. These errors leave uncertain the actual identification of each motor-unit firing instance and provide a measure of accuracy of the decomposition procedure.

For each motor-unit firing instance found in the EMG signal, the precise temporal localization of the MUAP is subject to variability. This variability gives rise to a second type of error that we refer to as Location error. For manual decomposition methods, noise embedded in the EMG signal can mask the precise location of each action-potential peak and therefore, the location of each firing instance. Whereas the resultant location error may be small when a single motor unit is present, the error increases with the superposition of two or more action potentials and increases further with a decreasing signal-to-noise ratio, as shown in Fig. 1B. For automated methods, decomposition of complex shapes from multiple superimposed action potentials can also result in location errors, as shown in Fig. 1C. Small shifts in the location of relatively high-amplitude MUAPs in the superposition subjugate relatively lower-amplitude MUAPs to larger shifts in their precise location.

Although considerable attention has been given to the study of identification errors, direct measurements of location errors have not been considered in previous studies (Holobar et al. 2010; Kleine et al. 2008; Marateb et al. 2011). In addition to the lack of a comprehensive evaluation of decomposition

Address for reprint requests and other correspondence: C. J. De Luca, NeuroMuscular Research Center, Boston Univ., 19 Deerfield St., Boston, MA 02215 (e-mail: cjd@bu.edu).

### Types of Decomposition Errors

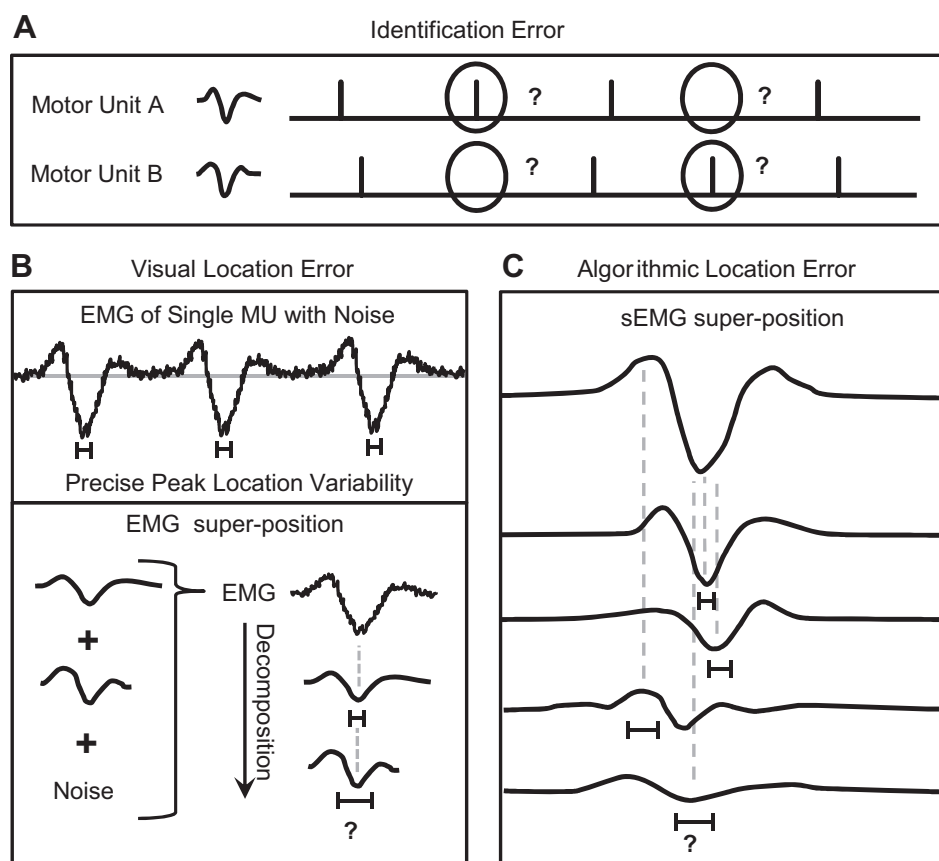


Fig. 1. Pictorial representation of errors made during electromyographic (EMG) decomposition. *A*: when the firing instances from 2 similarly shaped motor-unit action potentials (MUAPs) occur amongst certain superpositions or noise manifestations, mistakes are likely to occur in the form of misidentifications between the firing instances of 2 motor units. These “Identification errors” consist of either falsely detected or missed firing instances and are revealed by validation of the decomposition. *B*: any decomposition technique is also subject to “Location errors.” During manual decomposition, superposition of noise with even a single active MUAP (MU) can blur the precise location of the action-potential peak, giving rise to location variability during template matching, measured as a location error. The location error is magnified when a manual template-matching algorithm is applied to a superposition occurrence of 2 MUAPs, a common happening during even lowest-level contractions. *C*: in automated decomposition, location errors occur, due to the frequent incidence of complex superpositions in the EMG signal, the resolution of which gives rise to shifts in the precise location of MUAPs, often caused by distortions of the shapes remaining within the superposition during the subtraction process. Any noise in the EMG signal would only render more difficult the determination of the precise temporal location of each firing instance. sEMG, surface EMG.

errors, no systematic method has ever been proposed to mitigate the effects of errors on the extracted motor-unit firing instances. Instead, the majority of published studies resorts to discarding potentially erroneous data and in so doing, limits any analysis to sections of a select few MUAPTs.

Consequently, we set out to classify decomposition errors and develop an algorithm that reduces errors and improves the EMG signal-decomposition data. We studied errors made by our decomposition EMG (dEMG) algorithms, described by De Luca et al. (2006) and improved substantially by Nawab et al. (2010). The accuracy of our dEMG algorithms has been assessed using the decompose-synthesize-decompose-compare (DSDC) validation, described by Nawab et al. (2010). The efficacy of this validation approach has been questioned by Farina and Enoka (2011). We and others responded with evidential proof that the approach was efficacious and correct. De Luca and Contessa (2012) provided empirical evidence that the DSDC method is an unbiased method for measuring the accuracy of our dEMG algorithms. Subsequently, independent verification has been provided via three different methods. Hu et al. (2013a, b) confirmed that the MUAPs identified by our dEMG algorithms were similar in shape with those obtained by trigger averaging the MUAP from the sEMG signal. In a separate test, Hu et al. (2013a, c) demonstrated that the firing instances obtained by our dEMG algorithms were resolved accurately within 0.6–2.0 ms, and Hu et al. (2013b, 2014) provided visual verification that our dEMG algorithms yield MUAPTs with an average accuracy of 95%.

In the present study, we applied the DSDC validation to measure the errors made by our dEMG algorithms on a set of 1,061 MUAPTs. Although identification errors have been measured and reported in our previous publications, we expanded the error analysis in this study to include a thorough classification of location errors. After the measuring of decomposition errors, we proceeded to derive a new algorithm, capable of mitigating the errors and improving the decomposition result. The error-reduction algorithm combined multiple estimates of a recorded sEMG decomposition to obtain a more probable estimate of motor-unit firing instances with fewer errors. We evaluated the error-reduction algorithm using a set of sEMG signals synthesized from known MUAPTs and known firing instances and found that the decomposition errors were reduced effectively.

### METHODS

**Subjects.** Six healthy subjects, four men and two women, each with no known history of neuromuscular disorders, volunteered for the study. The average subject age was  $21.3 \pm 0.8$  yr and ranged from 21 to 23 yr. Before participating in the study, all subjects read, indicated they understood, and signed a consent form, approved by the Institutional Review Board at Boston University.

**Force measurements.** All experiments were performed on the first dorsal interosseus (FDI) muscle of the hand and the vastus lateralis (VL) muscle of the lower limb. Subjects were seated in a specially constructed chair apparatus designed to isolate movement for target muscles of this study. For the VL contractions, the chair restrained hip movement and immobilized the subject’s leg at a knee angle of  $60^\circ$

flexion. For the FDI, surface restraints were used to immobilize the subject's forearm and restrain the wrist and fingers. Isometric force was measured during leg extension and index-finger abduction via load cells attached to metal arms of each restraint. The force was band-pass filtered from 0 to 450 Hz and digitized at 20 kHz. Target trajectories and visual feedback of the isometric contraction force were displayed on a computer monitor for the subject.

**EMG signal recording.** The sEMG signals were recorded with a sensor containing five cylindrical pins, 0.5 mm in diameter, located at the corners and in the middle of a 5 × 5-mm square. Further details may be found in De Luca et al. (2006). The output of the sensor was connected to an EMG amplifier (a Bagnoli 16-channel system; Delsys, Natick, MA). Before application of the sensor to the subject, the surface of the skin was prepared by removing hair with a razor (which we no longer find necessary) and dead skin with adhesive tape, followed by sterilization of the skin with an alcohol cloth. After skin preparation, the surface sensor was placed on the skin over the center of the muscle belly. Signals from the four pairs of electrodes in the sensor were differentially amplified and filtered with a bandwidth of 20–450 Hz. The signals were sampled at 20 kHz and stored in a computer hard drive for offline data analysis.

**Experimental protocol.** Before recording data, subjects were trained on the protocol by practicing force tracking and maximal voluntary contractions (MVCs). Following training, we measured the MVC force by three brief MVCs, each with a 3-s duration, separated by a rest period of 3 min. The MVC of greatest value was chosen to normalize the force level of all following contractions for later comparison across subjects. Subjects proceeded to track a series of target trapezoidal trajectories displayed on the computer screen with the output of their force sensor. For the FDI muscle, trajectories increased at a rate of 10% MVC/s; were sustained at 5, 10, 15, 20, 25, or 30% MVC for 35 s; and were then decreased back to zero at 10% MVC/s. For the VL muscle, trajectories again increased at a rate of 10% MVC/s; were sustained at 20, 25, 30, 35, 40, or 50% MVC for 35 s; and were then decreased back to zero at 10% MVC/s. At least 5 min of rest was allotted between trials.

**EMG signal decomposition.** The sEMG signals recorded from four channels of the sensor were decomposed into their constituent MUAPs using the dEMG algorithms described by De Luca et al. (2006) and Nawab et al. (2010). The decomposition of the complex sEMG signal into MUAPs is a computationally expensive procedure in a multidimensional constraint space. To mitigate this computational challenge, we designed special artificial intelligence architecture to restrict the number of constraint combination searches by dividing the decomposition into a series of stages. Each processing stage addressed a fraction of the constraints of the decomposition problem. These stages did not use any assumptions of motor-unit firing properties. Instead, the algorithm generated MUAP candidates for given electrical events in the sEMG signal, only on the basis of the characteristics of the MUAP waveforms. In rare cases, when two different MUAP templates (typically among the smallest-sized templates with relatively “flat” shapes), as well as their slightly misaligned superposition, accounted equally well for a local shape within an electrical event, the algorithm used the principle of minimization of the interpulse interval coefficient of variation of each of the involved units to resolve the ambiguity. In our experience with the dEMG algorithm applied to real sEMG signals, <1% of the firing instances within a decomposition result was ever involved in this type of ambiguity resolution. For a more detailed description of the algorithm's functionality, refer to Nawab et al. (2008, 2010). The output of the algorithm provided the firing instances of all MUAPs that could be identified by the algorithm, a subset of the MUAPs that contributes to the energy of the sEMG signal. Any MUAPs or fragments of MUAPs that were not identified consistently were allocated to a residual signal. For each identified MUAP, the firing instance was taken as the time of the greatest absolute value of the MUAP shape.

**EMG validation.** We implemented the DSDC validation to measure the identification and the location errors. The identification errors, made for all firing instances of each MUAPT, were classified by the accuracy metric

$$Accuracy = 1 - Identification\ Errors = 1 - \frac{N_{error}}{N_{truth}} = 1 - \frac{N_{FP} + N_{FN}}{N_{TP} + N_{TN}} \quad (1)$$

Specifically, the number of errors ( $N_{error}$ ) was evaluated as the sum of the false-positive ( $N_{FP}$ ) and false-negative ( $N_{FN}$ ) firing instances detected. The number of true firing instances, or  $N_{truth}$ , was quantified as the number of true positives ( $N_{TP}$ ), or known firing instances, plus the number of true negatives ( $N_{TN}$ ), or regions in the known MUAPs containing no firing instances [see Appendix 1 in De Luca and Contessa (2012)].

The location errors were measured from firing instances that were identified successfully but with slight variability in their temporal location. Location errors were computed for all motor-unit firing instances as

$$\varepsilon_{i,j} = decomposed_{i,j} - known_{i,j} \quad (2)$$

where  $known_{i,j}$  is the known  $j^{th}$  firing instance of the  $i^{th}$  MUAPT, and  $decomposed_{i,j}$  is the  $j^{th}$  firing instance of the  $i^{th}$  MUAPT decomposed during the validation process. The location errors for each MUAPT were binned in histograms for further analysis. We quantified the total amount of location error for each MUAPT as

$$AM\{Location\ Error\}_i = \frac{1}{n} \sum_{j=1}^n |\varepsilon_{i,j}| \quad (3)$$

where  $AM\{Location\ Error\}_i$  is the average magnitude of the location error for all  $n$  firing instances in the  $i^{th}$  MUAPT.

**Error-reduction algorithm.** The basic concept of the error-reduction algorithm consisted of decomposing the recorded sEMG signal into multiple estimates of the constituent MUAPs and combining these estimates to derive a new estimate with fewer and smaller decomposition errors. To obtain multiple decomposition estimates, we repeated a process of generating a randomized noise signal, adding the noise to the recorded sEMG signal, and decomposing the resultant signal. Examples of multiple decomposition estimates of the same MUAPs are denoted in Fig. 2. For each decomposition repetition, the noise added to the sEMG signal was a random manifestation of band-limited Gaussian noise equal in root mean square (RMS) to the baseline noise in the recorded signal.

MUAPs from different motor units were identified across the decomposition estimates using a maximum likelihood estimator, based on the maximum a posteriori probability classifier, first described in LeFever and De Luca (1982a). In the current implementation for error reduction, the classifier remained agnostic to firing statistics. Instead, MUAPs, representing the activity of the same motor units across the different decomposition estimates, were identified, based solely on the characteristics of the MUAP waveforms [see Nawab et al. (2008) for more details]. The firing instances of several estimates of one MUAPT are shown in Fig. 3. For each MUAPT, all estimates of the same motor-unit firing instance were assigned an index  $j$ . The index of each firing instance was determined based on the temporal location of the firing instances from different decomposition estimates using a “nearest-neighbor” classifier. Specifically, firing instances from different decomposition estimates were given the same index  $j$ , if and only if the following two criteria were met: 1) the firing instance from a first decomposition estimate had to be the closest firing instance to the firing instance obtained from a second decomposition estimate, and 2) the firing instance from the second decomposition estimate had to be the closest firing instance to the firing instance obtained from the first decomposition estimate. The nearest-neighbor algorithm was repeated until all decomposition es-

**Error Reduction Procedure**

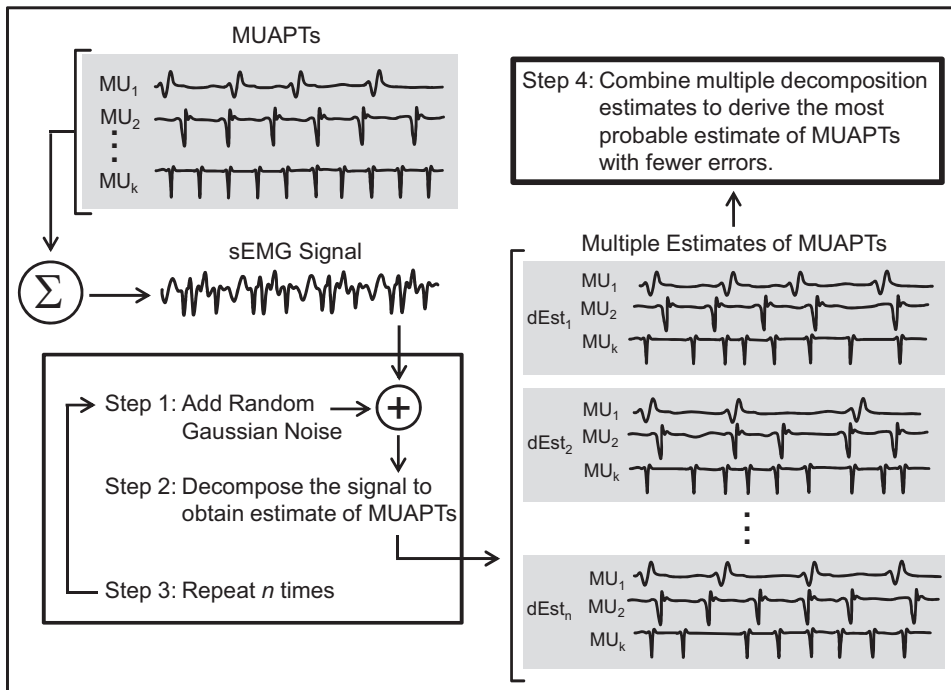


Fig. 2. A diagrammatic depiction of the process used to generate multiple decomposition estimates for error reduction. During voluntary contraction, MUAP trains (MUAPTs), denoted  $MU_k$ , were recorded in the sEMG signal. The signal was combined with randomized Gaussian noise and subsequently decomposed to obtain an estimate of the MUAPTs, denoted  $dEst_i$ . The process of randomizing the noise, adding it to the signal, and decomposing the signal was repeated  $n$  times to obtain  $n$  slightly different estimates of the MUAPTs. These decomposition estimates were then combined to obtain a more probable estimate of the MUAPTs within the synthesized signal.

imates of the same motor-unit firing instance were assigned the proper index.

The heart of the error-reduction algorithm consisted of decision criteria designed to establish the most probable identification and location of each motor-unit firing instance. For the identification decision, positive or negative identification of each firing instance was determined based on a 50% decision criteria: if  $>50\%$  of the decom-

position estimates identified the firing instance, then it was regarded as a positive identification; otherwise, it was considered a negative identification. For example, the firing instance, assigned  $t_4$  in Fig. 3, was identified in only one of the three decomposition estimates and was therefore marked as a negative identification. All positive identifications of firing instances were then applied to the location decision stage of error reduction. The location decision provided a new firing

**Error Reduction Algorithm**

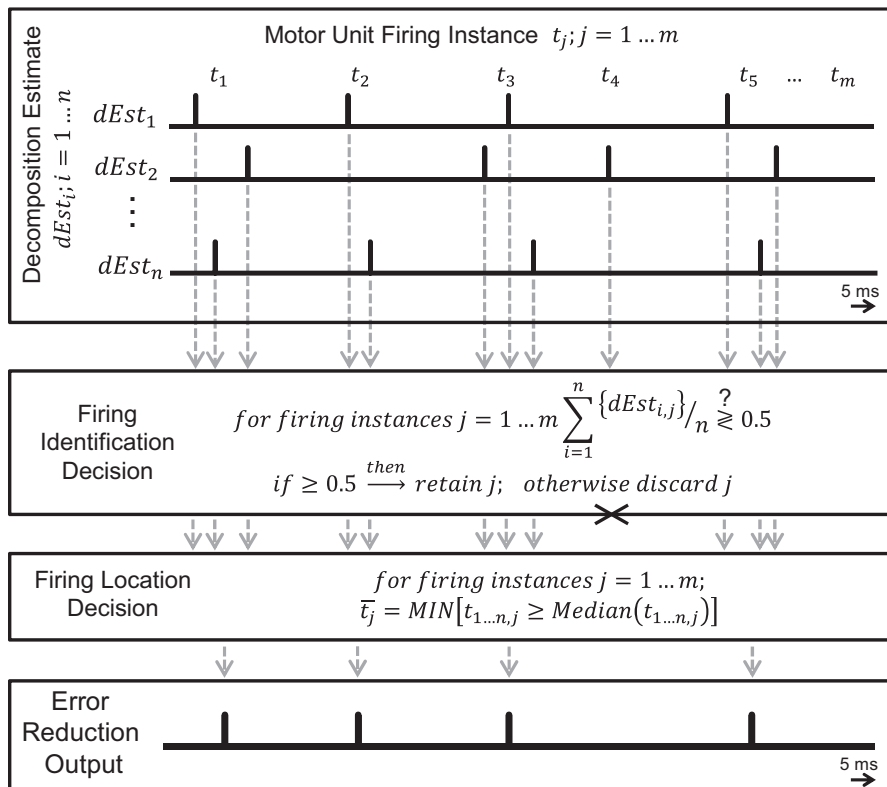


Fig. 3. The specific decision stages used in the error-reduction algorithm. Multiple decomposition estimates, denoted  $dEst_i$ , were obtained using the procedure illustrated in Fig. 2. Three example decomposition estimates of the same MUAPT are shown. Firing instances from different decomposition estimates that represented the same motor-unit firing instance were assigned an index  $j$ . To evaluate the firing identification, each  $j^{th}$  firing instance was regarded as a positive identification, if and only if the firing instance was identified in  $\geq 50\%$  of the  $i^{th}$  decomposition trials,  $dEst_{i,j}$ . For all positive identifications of firing instances, the location of the firing instance was decided as the 1st firing instance  $\geq$  median temporal location of all estimates of the firing instance,  $t_{1...n,j}$ . The final output of the error reduction provided a more probable estimate of the identification and location of each motor-unit firing instance.

instance equal to the first estimate of the firing instance greater than or equal to the median temporal location of all estimates of the firing instance. These new firing instances provided the final output of the error-reduction algorithm.

**Evaluating error reduction.** We evaluated the efficacy of the error-reduction algorithm using a process based on our DSDC validation approach. Multiple decomposition estimates were generated using the same procedure described in the error-reduction algorithm above, with two key differences.

1) Instead of using a recorded sEMG signal, we evaluated the error reduction by decomposing a synthesized sEMG signal. The synthesized signal was comprised of MUAPTs obtained from the decomposition of the recorded sEMG signal.

2) The noise added to the synthesized sEMG signal was similarly, randomly generated, band-limited Gaussian noise, but it was equal in RMS to the residual of the decomposition of the recorded sEMG signal (see EMG signal decomposition above).

As shown in Fig. 2, by repeating the steps of generating random noise, adding the noise to the synthesized signal, and decomposing the signal, we obtained multiple estimates of the MUAPTs.

With the use of the steps depicted in Fig. 3, a new estimate of the MUAPTs, with fewer decomposition errors with respect to the synthesized signal, was obtained by processing multiple decomposition estimates of the same MUAPTs. The new estimates of the MUAPTs, obtained from error reduction, were then compared with the actual MUAPTs known within the synthesized signal to evaluate the efficacy of the error-reduction process. MUAPTs obtained from error reduction were matched with the corresponding MUAPTs known within the synthesized signal by evaluating the similarity between the characteristic MUAP shapes using a maximum likelihood estimator. For each matched MUAPT, we paired the estimated motor-unit firing instances with the corresponding firing instances known within the synthesized signal, using a nearest-neighbor classifier. Any time difference between paired firing instances provided the location error, and location errors were computed for all matched firing instances using Eq. 2 and quantified for each MUAPT using Eq. 3. All unmatched firing instances were considered identification errors. We quantified the total amount of identification errors made for all firing instances of each MUAPT using the accuracy metric described in Eq. 1. Identification and location errors were measured after implementing the error-reduction algorithm with three to as many as 39 synthesized signal-decomposition estimates. This range of estimates was determined sufficient to reveal any reduction of errors while reducing the impractical computational expense of the procedure. The efficacy of the error-reduction algorithm was indicated by the improvements in accuracy (1.0 – proportion of identification errors) and reduction in location error.

## RESULTS

We collected and analyzed a data set from 36 voluntary isometric contractions, a subset of the 144 voluntary isometric contractions reported in the accompanying study by De Luca and Kline (2014). A total of 1,061 identified MUAPTs, containing 784,767 firing instances, was studied; 509,404 firing instances from 616 motor units were from the VL contractions, and 275,363 firing instances from 445 motor units were from the FDI contractions. The number of MUAPTs obtained from decomposition of the sEMG signal recorded during each contraction ranged from 17 to 51, with an average of 29. No correlations were found between the number of MUAPTs obtained and the force level or subject of each contraction. (Note that some of the identified MUAPTs may have been repetitions of the same motor unit observed in different contractions. Nonetheless, each identified MUAPT presented a unique challenge to the dEMG algorithms, due to the different

interaction of its differently represented action-potential shape and occurrences of superpositions, as each was encountered throughout the contraction.)

**Location errors.** With the use of the DSDC validation, we computed location errors of the firing instances obtained from decomposition. Four representative histograms of the magnitude of location errors are shown in Fig. 4 for two FDI and two VL MUAPTs. For each muscle, one histogram (Fig. 4, A and C) presents a relatively narrow range of location errors, and another (Fig. 4, B and D) presents a relatively wide range of location errors. These representative histograms exemplified the typical variability of the location-error data, measured from different MUAPTs. All histograms manifested a higher density of location errors near 0 ms, with progressively fewer errors at relatively greater temporal latencies. A qualitative comparison reveals no apparent distinction between location-error data from FDI contractions and VL contractions.

**Error-reduction results.** Error reduction was assessed using a set of synthesized signals with known firing instances. Figure 5 exemplifies changes in the accuracy (1.0 – proportion of identification errors) and location-error measurements, quantified for the firing instances of each MUAPT as the  $AM\{Location\ Error\}$ . Both error metrics are plotted as a function of the number of synthesized signal-decomposition estimates. Shown are errors from individual decomposition estimates of the synthesized sEMG signal and errors measured after combining the decomposition estimates in the error-reduction algorithm to form a new estimate. One motor unit with high initial accuracy and low initial  $AM\{Location\ Error\}$  is shown in Fig. 5, A and C, and another motor unit with low initial accuracy and high initial  $AM\{Location\ Error\}$  is shown in Fig. 5, B and D, respectively.

In all four plots, the combination of the decomposition estimates in the error-reduction algorithm resulted in lesser identification and location errors than were observed amongst the individual estimates. For instance, in one MUAPT with relatively high initial accuracy, the individual decomposition estimates varied between 97% and 98%, whereas error reduction improved the accuracy to >99%. For the same MUAPT, individual decomposition estimates produced  $AM\{Location\ Error\}$  values that varied between 3.8 ms and 4.5 ms, whereas error reduction decreased the  $AM\{Location\ Error\}$  of the firing instances to nearly 2.2 ms. Similar results are shown for the MUAPT, with a relatively low initial accuracy. Individual decomposition estimates varied in accuracy from 89.4% to 94.3% and in  $AM\{Location\ Error\}$  from 7.2 ms to 10.0 ms. However, error reduction for this MUAPT improved the accuracy to >97% and reduced the  $AM\{Location\ Error\}$  to ~6.1 ms.

A summary of the reduction in decomposition errors for the entire set of 1,061 MUAPTs is provided in Fig. 6 and Table 1. Histograms of the accuracy, location error, and mean firing rate are shown for the decomposition estimates before and after error reduction. Error reduction improved the average accuracy of all MUAPTs from 95.3% to 97.0% and improved the lower 95% confidence interval of the accuracy from 81.9% to 93.5% (compare Fig. 6, A with C). For location-error data, error reduction improved the  $AM\{Location\ Error\}$  from 5.10 ms to 3.44 ms on average (compare Fig. 6, B with D). Overall, improvements in accuracy were observed in 96.1% of MUAPTs, whereas reductions in  $AM\{Location\ Error\}$  were

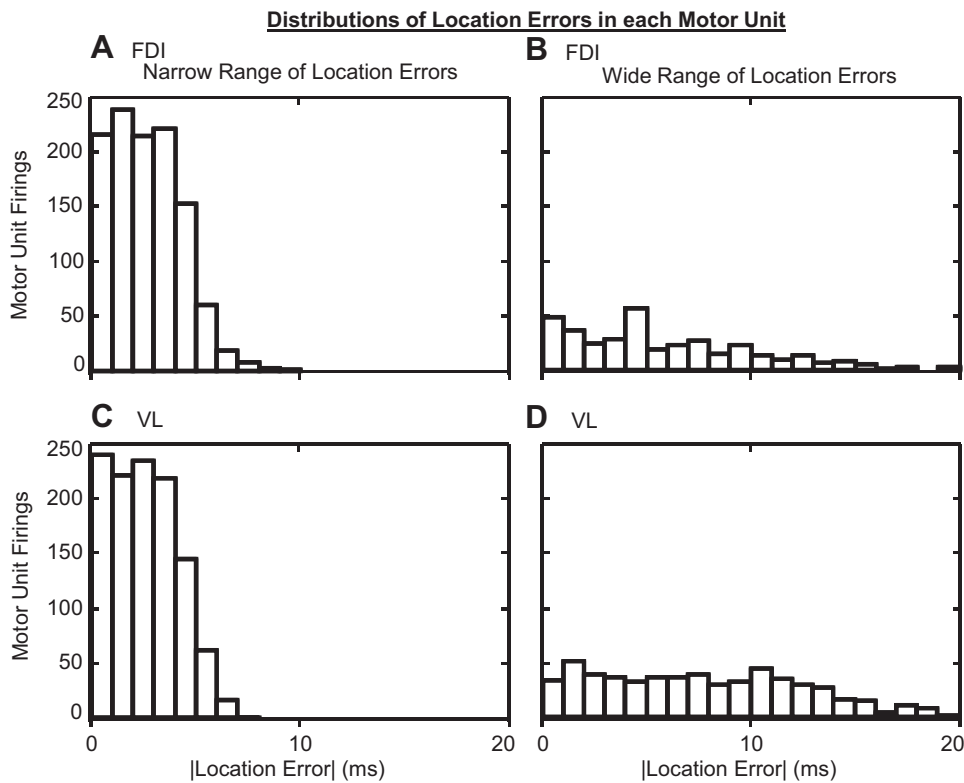


Fig. 4. Histograms of the location-error magnitude are shown in 1 ms bins for all firing instances of 1st dorsal interosseous (FDI) motor units with a (A) narrow and (B) wide range of location errors and for all firing instances of vastus lateralis (VL) motor units with a (C) narrow and (D) wide range of location errors.

seen in 100% of MUAPTs. Yet, on average, the mean firing rates of motor units remained largely unaffected by the error-reduction process. These data demonstrate that the error-reduction algorithm identified and mitigated decomposition errors successfully.

To study the performance characteristics of the error-reduction algorithm, we evaluated the percent of total MUAPTs found above different accuracy thresholds as a function of the number of estimates and the total time used for error reduction (Fig. 7). The time to decompose the different numbers of

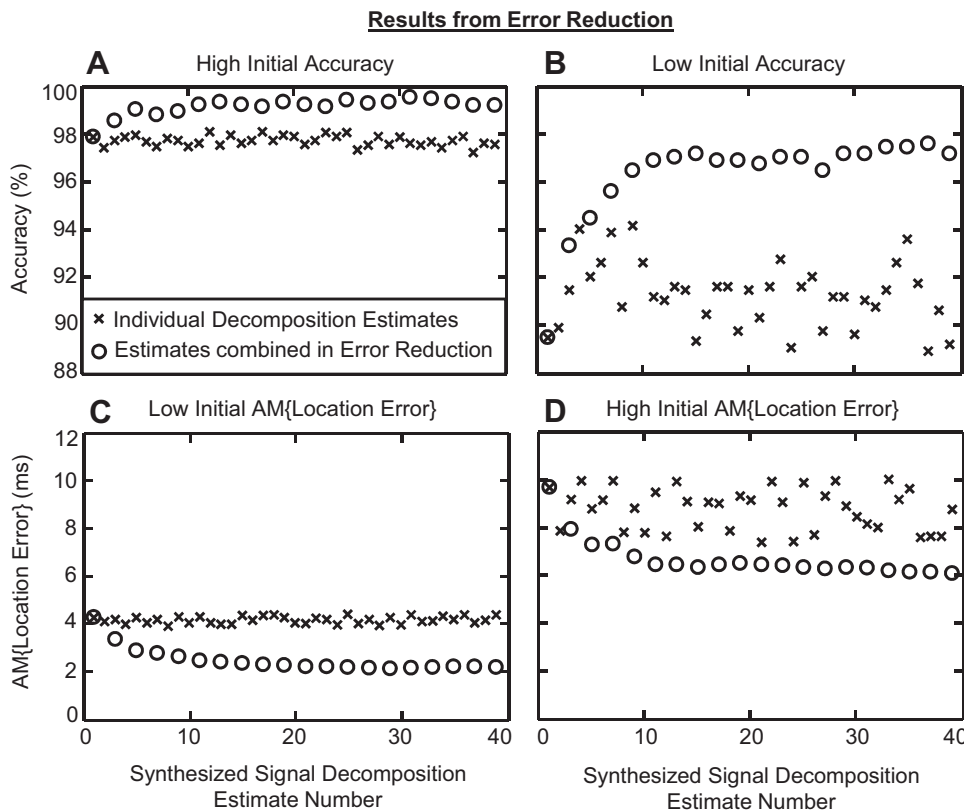


Fig. 5. The errors measured from multiple decompositions of synthesized sEMG signals are plotted as a function of the decomposition estimate number. Points plotted as "x" indicate errors measured from each of the individual, synthesized signal-decomposition estimates; points plotted as "o" indicate the errors measured from the output of error reduction, using the given number of synthesized signal-decomposition estimates. Accuracy data (1.0 = proportion of identification errors) are plotted for (A) 1 MUAPT with a relatively high initial accuracy and (B) 1 with a relatively low initial accuracy. The average magnitude of the location-error ( $AM\{Location\ Error\}$ ) data is plotted for the same MUAPTs: (C) 1 with a relatively low initial  $AM\{Location\ Error\}$  and (D) another with a relatively high initial  $AM\{Location\ Error\}$ . The individual decomposition estimates manifested accuracy and  $AM\{Location\ Error\}$  values that were minimally distributed around a central mean. However, the combination of the individual estimates in the error-reduction algorithm produced new estimates with increased accuracy and decreased location-error values.

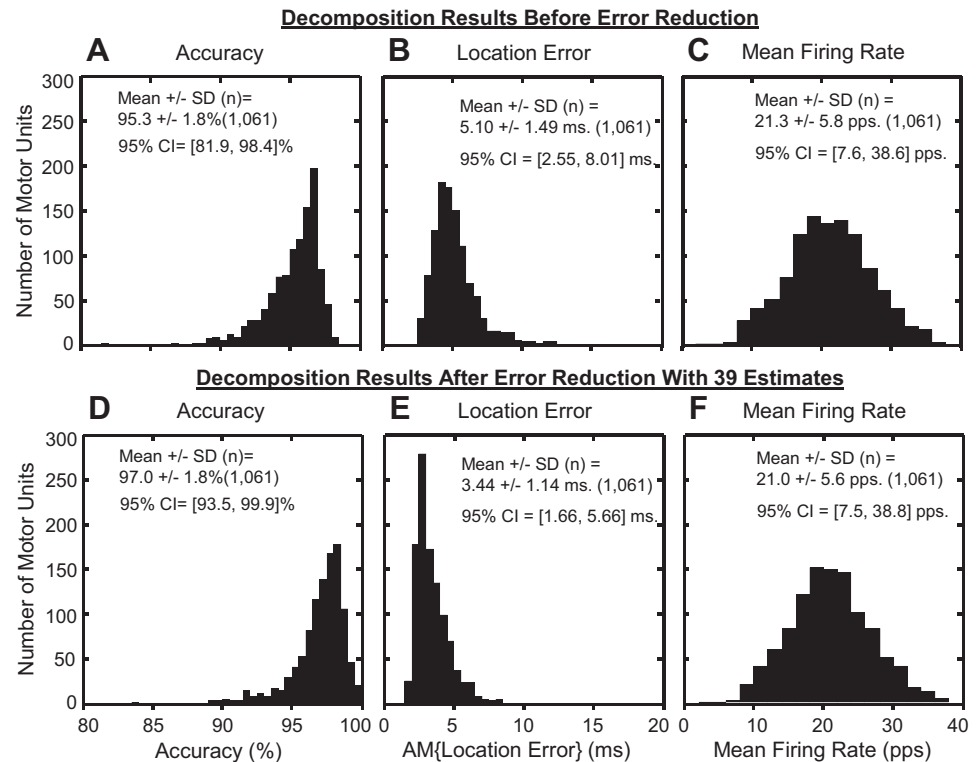


Fig. 6. Histograms showing distributions of the (A and D) accuracy (1.0 – proportion of identification errors), (B and E)  $AM\{Location\ Error\}$ , and (C and F) mean firing rate of motor units computed from (A–C) a single decomposition estimate of the synthesized signals and (D–F) the result of error reduction using 39 synthesized signal-decomposition estimates. On average, the error-reduction algorithm improved the accuracy and reduced the location-error values, whereas mean firing rates remained largely unaffected. CI, confidence interval; pps., pulses/s.

estimates was based on a personal computer with an Intel Core i5-2500 3.3 GHz processor and 4 gigabytes of memory, running a Windows 7 Enterprise 64-bit operating system. The exact computational time required to evaluate specific numbers of estimates for error reduction will vary with the hardware and software capabilities of different computers. Three different accuracy thresholds (95, 97, and 98%) are shown in Fig. 7, *top*. Generally, the percentage of MUAPTs above each accuracy threshold increased with an increasing number of estimates. For example, <20% of 1,061 MUAPTs were assessed above 97% accuracy, before mitigating errors. However, error reduction, using just nine estimates, increased the yield above the 97% accuracy threshold to >50%. For all accuracy thresholds, the yield of MUAPTs levels out with increasing numbers of estimates.

Similar results are shown for the percentage of MUAPTs obtained below a given  $AM\{Location\ Error\}$  threshold, also plotted as a function of the number of estimates and the total time required for error reduction. Three different  $AM\{Location\ Error\}$

Table 1. Summary of the results from the error-reduction algorithm

	MUAPTs	Mean $\pm$ SD	95% CI
Accuracy improvement	96.1% (1,020/1,061)	1.78 $\pm$ 1.10%	[0.05, 3.92]%
$AM\{Location\ Error\}$ reduction	100% (1,061/1,061)	1.66 $\pm$ 0.62 ms	[0.48, 2.87] ms

The improvements in accuracy (1.0 – proportion of identification errors) and reduction in average magnitude of the location error ( $AM\{Location\ Error\}$ ), computed for our entire data set of 1,061 motor-unit action-potential trains (MUAPTs), obtained from error reduction, using 39 synthesized signal-decomposition estimates. Shown are the percentage of MUAPTs with fewer decomposition errors, as well as the mean, SD, and 95% confidence interval (CI) of the improvement in accuracy and reduction in  $AM\{Location\ Error\}$ .

$Error\}$  thresholds (5, 4, and 3 ms) are shown in Fig. 7, *bottom*. The percentage of MUAPTs below each  $AM\{Location\ Error\}$  threshold increased with an increasing number of estimates used for error reduction. For example, the use of nine estimates for error reduction increased the yield of MUAPTs with <4 ms of  $AM\{Location\ Error\}$  from 20% to >60%. Similar to the accuracy data at all  $AM\{Location\ Error\}$  thresholds, the yield of MUAPTs levels out with increasing numbers of estimates.

## DISCUSSION

The error-reduction algorithm improved the estimates of the firing instances by combining multiple estimates obtained from the decomposition of the same sEMG signal with additive noise. On average, the accuracy (1.0 – proportion of identification errors) was improved in 96.1% of MUAPTs, and the  $AM\{Location\ Error\}$  was reduced in 100% of MUAPTs tested (see Table 1). As expected, the degree of error reduction increased with the number of decompositions performed and the consequential processing time. The operating point of the algorithm can be set to suit the requisite average accuracy level. The greater the error reduction required, the greater the number of iterations necessary and the longer the computational time. The trade-off among these variables may be seen in Fig. 7.

*Relevance of error reduction.* Any measurements of the properties of individual firing instances, such as synchronization or firing instance statistics, would be distorted by the errors inherent in any decomposition procedure. Whereas for the analysis of average motor-unit firing properties, such as the mean firing rates, the errors made by our dEMG algorithms minimally affect the values, because the errors in different firing instances are, in large part, independent of each other. Thus motor-unit firing instances are equally likely to have

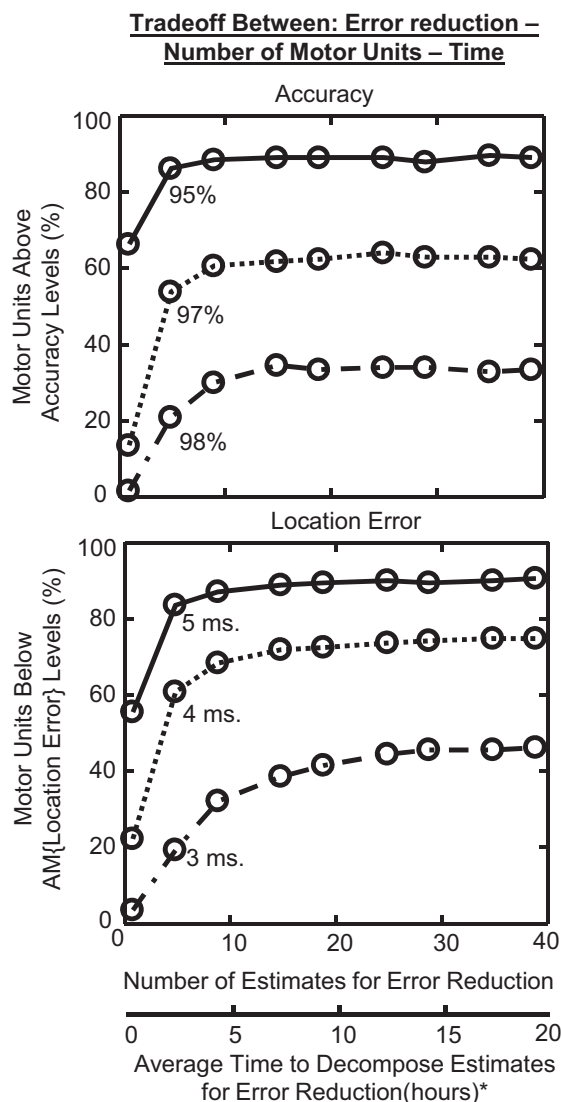


Fig. 7. Results illustrating the trade-off between the time required to obtain the specified number of decomposition estimates for error reduction and the number of MUAPTs obtained (*top*) above a given accuracy (1.0 – proportion of identification errors) threshold and (*bottom*) below a given  $AM\{Location\ Error\}$  threshold. The percent of 1,061 MUAPTs processed by the error-reduction algorithm is plotted for 3 different accuracy thresholds: 95% (solid line), 97% (dotted line), and 98% (dot-dash line) and 3 different  $AM\{Location\ Error\}$  thresholds: 5 ms (solid line), 4 ms (dotted line), and 3 ms (dot-dash line). The number of estimates used for error reduction to obtain the specific percentage of MUAPTs is plotted on the *x*-axis. Below the *x*-axis is another axis displaying the average time required to decompose the specified number of estimates. \*The processing time is based on a Lenovo ThinkCentre computer with an Intel Core i5-2500 3.3 GHz processor and 4 gigabytes of memory, running a Windows 7 Enterprise 64-bit operating system, and averages out to  $\sim 30$  min/estimate. Generally, more MUAPTs were obtained at higher accuracy and lower  $AM\{Location\ Error\}$  levels only at the expense of a greater processing time required to decompose additional estimates for error reduction.

false-positive or false-negative identification errors, as well as positive or negative location errors. Hence, as demonstrated by Fig. 6, *C* and *F*, the mean firing rate remains, in large part, immune to decomposition errors.

In the majority of previous studies, decomposition errors typically have been addressed by discarding potentially erroneous data. For example, in their analysis of motor-unit syn-

chronization, Nordstrom et al. (1992) were unable to resolve superposition occurrences in the EMG data, resulting in occasional missed firing instances. They argued that missed firing instances caused unusual and relatively high interpulse intervals. Therefore, to address the errors, they discarded all firing instances that produced interpulse intervals outside of an expected range. In spite of the obvious dangers associated with data selectivity, this strategy has been adopted widely throughout the synchronization literature (Dartnall et al. 2008; Hockensmith et al. 2005; Keen et al. 2012; Keen and Fuglevand 2004), without ever accounting for the effects of discarding data on subsequent measurements of synchronization.

The error-reduction algorithm is not limited to our dEMG algorithms. It can be applied to any decomposition procedure ranging from manual template-matching to automated methods. One example application could be for manual decomposition using visual template-matching with multiple human operators. After obtaining a first decomposition result, the resultant MUAPTs could be summed together; combined with randomly generated, band-limited Gaussian noise equal in RMS to the residual of the first decomposition; and subsequently, decomposed by a different human operator. The repetition of the synthesize-and-decompose steps across different human operators would yield multiple estimates of the first decomposition result. Such an implementation would allow for a better understanding of the types of errors made by humans during manual decomposition and the confidence with which manual decomposition results can be reported. Data so presented would provide a more reliable basis for describing the behavior of firing instances.

*Assessment of errors in decomposition algorithms.* Any procedure, manual or automatic, used to decompose EMG signals can only provide an estimate of the firing instances of the MUAPs within the signal. The accuracy of the estimate is affected by, among other factors, the complexity of the signal. Hence, the degree of the accuracy will depend on the soundness of the decomposition algorithm. In turn, the verification of the accuracy of the decomposition relies on other procedures and other algorithms. The quality and usefulness of these procedures and algorithms will establish the validity of the decomposition.

In this work, proof of the error-reduction algorithm relies on the use of the DSDC validation method that we have described in our previous work (De Luca and Contessa 2012; De Luca and Nawab 2011; Nawab et al. 2010). Farina and Enoka (2011) have questioned the validity of our DSDC method. Instead, they rely on validating the accuracy of the decomposition by using two alternative approaches: the two-source method and the mathematically synthesized signal method. Both methods were introduced and used by Mambrito and De Luca (1984), but we now know that they are susceptible to several drawbacks.

The two-source technique compares the MUAPTs of the same motor unit obtained from decomposition of two EMG signals recorded simultaneously with two sensors arranged in near proximity. Although it has been applied by De Luca et al. (2006), Holobar et al. (2009, 2012b, 2014), Hu et al. (2014), and Marateb et al. (2011), the MUAPTs in common, found in both sensor sources, are limited, typically ranging from one to three (De Luca et al. 2006; Hu et al. 2014). Hence, the accuracies of the rest of the MUAPTs, obtained from decom-

position, remain untested, thereby requiring the application of an additional validation technique.

The second validation approach consisted of using a mathematically synthesized signal with known MUAP shapes and firing instances that are designated as the “truth.” The mathematically synthesized signal is decomposed, and the accuracy is evaluated by comparing the truth data with the decomposed data. This method has been used by Farina and Merletti (2001), Florestal et al. (2006), Holobar et al. (2009), and Zennaro et al. (2003). Although this is a classical engineering approach, it has limitations for establishing the accuracy of individual MUAPTs extracted from real sEMG signals.

1) It requires the presumption that the accuracy results obtained under artificial conditions provide a faithful representation of the decomposition accuracy of a real sEMG signal. This is a difficult point to establish.

2) It is a subjective approach, as the parameters of the firing instances are constructed artificially, as was done by Holobar et al. (2012a) and Holobar and Zazula (2007), or are derived from a generic model, such as the model reported by Fuglevand et al. (1993).

Recent attempts to overcome these drawbacks have led to the development of two alternative validation methods. McGill and Marateb (2011) and Parsaei and Stashuk (2013) estimated the decomposition accuracy using statistical assumptions of MUAPTs, including the following: 1) independent motor-unit firing instances and 2) stationary MUAP shapes throughout the duration of a contraction. However, dependence between MUAPTs in the form of synchronized firing instances (Kamen and Roy 2000; Keen et al. 2012; Nordstrom et al. 1992) and correlated fluctuations in their firing rates, known as “common drive” (De Luca and Erim 1994; De Luca et al. 1982; Farina et al. 2014; Laine et al. 2013), are well documented in the literature. With respect to the stationarity of the individual MUAPTs, Bertram et al. (1995), De Luca (1984), Fortune and Lowery (2009), Juel (1988), and Roy et al. (2007) have observed that the shapes of individual MUAPs are not stationary throughout a contraction.

As an alternative, Farina et al. (2014) and Holobar et al. (2014) reported that the accuracy of their convolution kernel compensation (CKC) decomposition algorithm could be estimated by the ratio of the MUAP signal energy to the energy of the sEMG noise, a metric they referred to as the pulse-to-noise ratio. However, in the contractions they studied, as much as 50% of the variability in the decomposition sensitivity (a measure of some identification errors) was not correlated with the pulse-to-noise ratio.

Our DSDC validation was designed to improve upon other validation approaches. It has five elements that support its reliability and soundness.

1) Our validation uses a synthesized sEMG signal, but unlike the mathematically synthesized signal used by others, ours is a realistic-synthesized sEMG signal that is of the same class as the real sEMG signal. It is constructed with the MUAP shapes and firing instances of the decomposed real sEMG signal [see Nawab et al. (2010) for details].

2) Direct empirical tests have shown that our DSDC validation method does not produce biased results. De Luca and Contessa (2012) demonstrated that the decomposition accuracy measured using a signal synthesized from MUAPs with randomized firing times was 95.4%, virtually identical to the

95.6% accuracy measured using a signal synthesized from the same MUAPs but with firing times provided by our dEMG algorithm.

3) The DSDC algorithm evaluates the accuracy and location errors for a complete set of MUAPTs obtained from the decomposition of a real sEMG signal. This compares with only one to three MUAPTs typically assessed using the two-source test.

4) Our validation algorithm matches firing instances obtained from decomposition with firing instances known within the synthesized signal, using a nearest-neighbor classifier instead of an arbitrarily predetermined range of temporal variability. Therefore, we can obtain a reliable measure of the location error with which the firing instances of each MUAPT are resolved.

5) Our test is universal. It can be applied to a variety of decomposition methods ranging from manual to automated algorithms.

Therefore, the thorough assessment provided by the DSDC validation, coupled with the extensive, independent verification by Hu et al. (2013a, b, c, 2014), demonstrates that our dEMG algorithms can extract the likely physiological MUAPs from unique and complex superpositions throughout the sEMG signal to the extent of the accuracy and location-error measurements we report.

*Consideration of location errors.* The DSDC validation was successful in measuring the location errors made by our dEMG algorithms. It was tested on 784,767 motor-unit firing instances from 36 contractions of the VL and FDI muscles. No apparent difference existed between location-error histograms from MUAPTs of FDI contractions and those of VL contractions (Fig. 4). The location error was quantified for all firing instances of each motor unit as the  $AM\{Location\ Error\}$  and averaged 5.10 ms for all 1,061 validated MUAPTs, as shown in Fig. 6B.

In the past, the problem of measuring the location error has been given little consideration. Studies by Bigland-Ritchie et al. (1983), Enoka et al. (1989), Keen and Fuglevand (2004), and Nordstrom et al. (1992) provide no account of location errors made during manual decomposition of indwelling EMG signals. Even if only a single motor unit were active, the superposition of an individual action potential with baseline and ambient noise can yield uncertainty in the precise firing instance on the order of a few milliseconds. For instance, McGill et al. (2004) reported that motor-unit firing instances, decomposed manually from indwelling EMG signals, can range in temporal location by as much as 5 ms.

Studies using sEMG signal decomposition have also omitted direct measurements of location errors. Instead, any motor-unit firing instances validated outside of an arbitrary range of temporal location have been considered as false detections by Holobar et al. (2010), Kleine et al. (2008), and Marateb et al. (2011). Although this approach has some usefulness for indicating bounds of the temporal variability of some firing instances, it provides no account of the actual MUAP location errors made during decomposition. The approach can be problematic when firing instances outside of the temporal location range are excluded from analysis [for example, see Marateb et al. (2011)].

*Consideration of identification errors.* We quantified identification errors using an accuracy metric (1.0 – proportion of

identification errors) for all firing instances of each MUAPT (refer to Eq. 1). More than 66% of all 1,061 MUAPTs were obtained with >95% accuracy. On average, 29 MUAPTs were found in the sEMG signal from each contraction, and the average accuracy was 95.3% (see Fig. 6A).

Other studies have addressed the issue of identification errors using measures that favored expediency. For example, Marateb et al. (2011) only measured errors from a portion of motor-unit firing instances that was considered “highly confident” from each MUAPT. From this subset, they reported an average accuracy of 91.5%. In another verification study, Holobar et al. (2009) used a metric of sensitivity to quantify identification errors made when decomposing a simulated sEMG signal and reported values >95%. However, measures of sensitivity only account for false-negative identification errors. If false positives were also included in their calculations, then the actual accuracy of their decomposition results would likely be lower. More recently, Holobar et al. (2012b) quantified identification errors made by their CKC algorithm using the two-source technique. The “rate of agreement” between the firing instances obtained from indwelling EMG signals and those obtained by their CKC algorithm from sEMG signals ranged from 89% to 100%. However, their analysis only included a select subset of MUAPTs that they considered had a “highly regular discharge pattern.” When a relatively larger set of MUAPTs was assessed by Holobar et al. (2014), the rate of agreement was as low as 50%.

In this work, we have derived an algorithm that reduces the identification errors and the location errors of the firing instances of MUAPs extracted from the sEMG signal by a process of decomposition. The improved accuracy of the measured firing instances provides a more faithful expression of the firing instances of MUAPs in the real sEMG signal.

#### ACKNOWLEDGMENTS

We extend our gratitude to Dr. S Hamid Nawab for several useful discussions. We are also grateful to Dr. S. S. Chang for contributing to the development of the algorithms used to decompose and validate the sEMG signals and for assisting in the data processing. We thank the subjects who painstakingly participated in the experiments.

#### GRANTS

Support for this work was provided, in part, by the National Institute of Child Health and Human Development (HD05011/HD/NICHD) and National Institute of Neurological Disorders and Stroke (NS077526-01/NS/NINDS) and by funds from Delsys.

#### DISCLOSURES

C. J. De Luca is the president and CEO of Delsys, the company that developed the sEMG decomposition technology.

#### AUTHOR CONTRIBUTIONS

Author contributions: J.C.K. and C.J.D.L. conception and design of research; J.C.K. performed experiments; J.C.K. analyzed data; J.C.K. and C.J.D.L. interpreted results of experiments; J.C.K. prepared figures; J.C.K. and C.J.D.L. drafted manuscript; J.C.K. and C.J.D.L. edited and revised manuscript; J.C.K. and C.J.D.L. approved final version of manuscript.

#### REFERENCES

Bertram MF, Nishida T, Minioka MM, Janssen I, Levy CE. Effects of temperature on motor unit action potentials during isometric contraction. *Muscle Nerve* 18: 1443–1446, 1995.

- Bigland-Ritchie B, Johansson R, Lippold OC, Smith S, Woods JJ. Changes in motoneurone firing rates during sustained maximal voluntary contractions. *J Physiol* 340: 335–346, 1983.
- Dartnall TJ, Nordstrom MA, Semmler JG. Motor unit synchronization is increased in biceps brachii after exercise-induced damage to elbow flexor muscles. *J Neurophysiol* 99: 1008–1019, 2008.
- De Luca CJ. Myoelectrical manifestations of localized muscular fatigue. *Crit Rev Biomed Eng* 11: 251–279, 1984.
- De Luca CJ, Adam A, Wotiz R, Gilmore LD, Nawab SH. Decomposition of surface EMG signals. *J Neurophysiol* 96: 1646–1657, 2006.
- De Luca CJ, Contessa P. Hierarchical control of motor units in voluntary contraction. *J Neurophysiol* 107: 178–195, 2012.
- De Luca CJ, Erim Z. Common drive of motor units in regulation of muscle force. *Trends Neurosci* 17: 299–305, 1994.
- De Luca CJ, Kline JC. Statistically rigorous calculations do not support common input and long-term synchronization of motor unit firings. *J Neurophysiol*. First published September 10, 2014; doi: 10.1152/jn.00725.2013.
- De Luca CJ, LeFever RS, McCue MP, Xenakis AP. Control scheme governing concurrently active human motor units during voluntary contractions. *J Physiol* 329: 129–142, 1982.
- De Luca CJ, Nawab SH. Reply to Farina and Enoka: the reconstruct-and-test approach is the most appropriate validation for surface EMG signal decomposition to date. *J Neurophysiol* 105: 983–984, 2011.
- Enoka RM, Robinson GA, Kossev AR. Task and fatigue effects on low-threshold motor units in human hand muscle. *J Neurophysiol* 62: 1344–1359, 1989.
- Farina D, Enoka RM. Surface EMG decomposition requires an appropriate validation. *J Neurophysiol* 105: 981–982, 2011.
- Farina D, Merletti R. A novel approach for precise simulation of the EMG signal detected by surface electrodes. *IEEE Trans Biomed Eng* 48: 637–646, 2001.
- Farina D, Rehbaum H, Holobar A, Vujaklija I, Jiang N, Hofer C, Salminger S, van Vliet HW, Aszmann OC. Noninvasive, accurate assessment of the behavior of representative populations of motor units in targeted reinnervated muscles. *IEEE Trans Neural Syst Rehabil Eng* 22: 810–819, 2014.
- Florestal JR, Mathieu PA, Malanda A. Automated decomposition of intramuscular electromyographic signals. *IEEE Trans Biomed Eng* 53: 832–839, 2006.
- Fortune E, Lowery MM. Effect of extracellular potassium accumulation on muscle fiber conduction velocity: a simulation study. *Ann Biomed Eng* 37: 2105–2117, 2009.
- Fuglevand AJ, Winter DA, Patla AE. Models of recruitment and rate coding organization in motor-unit pools. *J Neurophysiol* 70: 2470–2488, 1993.
- Hockensmith GB, Lowell SY, Fuglevand AJ. Common input across motor nuclei mediating precision grip in humans. *J Neurosci* 25: 4560–4564, 2005.
- Holobar A, Farina D, Gazzoni M, Merletti R, Zazula D. Estimating motor unit discharge patterns from high-density surface electromyogram. *Clin Neurophysiol* 120: 551–562, 2009.
- Holobar A, Glaser V, Gallego JA, Dideriksen JL, Farina D. Non-invasive characterization of motor unit behaviour in pathological tremor. *J Neural Eng* 9: 1–13, 2012a.
- Holobar A, Minetto MA, Botter A, Farina D. Identification of motor unit discharge patterns from high-density surface EMG during high contraction levels. *5th European Conference of the International Federation for Medical and Biological Engineering Proceedings*. Berlin, Heidelberg: Springer, 2012b, 37, p. 1165–1168.
- Holobar A, Minetto MA, Botter A, Negro F, Farina D. Experimental analysis of accuracy in the identification of motor unit spike trains from high-density surface EMG. *IEEE Trans Neural Syst Rehabil Eng* 18: 221–229, 2010.
- Holobar A, Minetto MA, Farina D. Accurate identification of motor unit discharge patterns from high-density surface EMG and validation with a novel signal-based performance metric. *J Neural Eng* 11: 1–11, 2014.
- Holobar A, Zazula D. Multichannel blind source separation using convolution kernel compensation. *IEEE Trans Signal Process* 55: 4487–4496, 2007.
- Hu X, Rymer WZ, Suresh NL. Accuracy assessment of a surface electromyogram decomposition system in human first dorsal interosseus muscle. *J Neural Eng* 11: 026007, 2014.
- Hu X, Rymer WZ, Suresh NL. Assessment of validity of a high-yield surface electromyogram decomposition. *J Neuroeng Rehabil* 10: 99, 2013a.

- Hu X, Rymer WZ, Suresh NL.** Motor unit pool organization examined via spike triggered averaging of the surface electromyogram. *J Neurophysiol* 110: 1205–1220, 2013b.
- Hu X, Rymer WZ, Suresh NL.** Reliability of spike triggered averaging of the surface electromyogram for motor unit action potential estimation. *Muscle Nerve* 48: 557–570, 2013c.
- Juel C.** Muscle action potential propagation velocity changes during activity. *Muscle Nerve* 11: 714–719, 1988.
- Kamen G, Roy A.** Motor unit synchronization in young and elderly adults. *Eur J Appl Physiol* 81: 403–410, 2000.
- Keen DA, Chou LW, Nordstrom MA, Fuglevand AJ.** Short-term synchrony in diverse motor nuclei presumed to receive different extents of direct cortical input. *J Neurophysiol* 108: 3264–3275, 2012.
- Keen DA, Fuglevand AJ.** Common input to motor neurons innervating the same and different compartments of the human extensor digitorum muscle. *J Neurophysiol* 91: 57–62, 2004.
- Kleine BU, van Dijk JP, Lapatki BG, Zwartz MJ, Stegeman DF.** Using two-dimensional spatial information in decomposition of surface EMG signals. *J Electromyogr Kinesiol* 17: 535–548, 2007.
- Kleine BU, van Dijk JP, Zwartz MJ, Stegeman DF.** Inter-operator agreement in decomposition of motor unit firings from high-density surface EMG. *J Electromyogr Kinesiol* 18: 652–661, 2008.
- Laine CM, Negro F, Farina D.** Neural correlates of task-related changes in physiological tremor. *J Neurophysiol* 110: 170–176, 2013.
- LeFever RS, De Luca CJ.** A procedure for decomposing the myoelectric signal into its constituent action potentials—part I: technique, theory and implementation. *IEEE Trans Biomed Eng* 29: 149–157, 1982a.
- LeFever RS, De Luca CJ.** A procedure for decomposing the myoelectric signal into its constituent action potentials—part II: execution and test for accuracy. *IEEE Trans Biomed Eng* 29: 158–164, 1982b.
- Mambrito B, De Luca CJ.** A technique for the detection, decomposition and analysis of the EMG signal. *Electroencephalogr Clin Neurophysiol* 58: 175–188, 1984.
- Marateb HR, McGill KC, Holobar A, Lateva ZC, Mansourian M, Merletti R.** Accuracy assessment of CKC high-density surface EMG decomposition in biceps femoris muscle. *J Neural Eng* 8: 1–11, 2011.
- McGill KC, Lateva ZC, Johanson ME.** Validation of a computer-aided EMG decomposition method. *Conf Proc IEEE Eng Med Biol Soc* 7: 4744–4747, 2004.
- McGill KC, Marateb HR.** Rigorous a posteriori assessment of accuracy in EMG decomposition. *IEEE Trans Neural Syst Rehabil Eng* 19: 54–63, 2011.
- Nawab SH, Chang SS, De Luca CJ.** High-yield decomposition of surface EMG signals. *Clin Neurophysiol* 121: 1602–1615, 2010.
- Nawab SH, Wotiz RP, De Luca CJ.** Decomposition of indwelling EMG signals. *J Appl Physiol* 105: 700–710, 2008.
- Nordstrom MA, Fuglevand AJ, Enoka RM.** Estimating the strength of common input to human motoneurons from the cross-correlogram. *J Physiol* 453: 547–574, 1992.
- Parsaei H, Stashuk DW.** EMG signal decomposition using motor unit potential train validity. *IEEE Trans Neural Syst Rehabil Eng* 21: 265–274, 2013.
- Roy SH, De Luca G, Cheng MS, Johansson A, Gilmore LD, De Luca CJ.** Electro-mechanical stability of surface EMG sensors. *Med Biol Eng Comput* 45: 447–457, 2007.
- Zennaro D, Wellig P, Koch VM, Moschytz GS, Läubli T.** A software package for the decomposition of long-term multichannel EMG signals using wavelet coefficients. *IEEE Trans Biomed Eng* 50: 58–69, 2003.

